Impact of Quaternary-Pumped Storage Hydropower on Frequency Response of U.S. Western Interconnection with High Renewable Penetrations

Preprint

Soumyadeep Nag,[1,2] Zerui Dong,[3] Jin Tan,[1] Jinho Kim,[3] Eduard Muljadi,[3] Kwang Y. Lee,[2] and Mark Jacobson[1]

1 National Renewable Energy Laboratory
2 Baylor University
3 Auburn University

Presented at the 2022 IEEE Power and Energy Society General Meeting
Denver, Colorado
July 17–21, 2022

NREL is a national laboratory of the U.S. Department of Energy
Office of Energy Efficiency & Renewable Energy
Operated by the Alliance for Sustainable Energy, LLC

This report is available at no cost from the National Renewable Energy Laboratory (NREL) at www.nrel.gov/publications.

Contract No. DE-AC36-08GO28308

Conference Paper
NREL/CP-6A40-81418
July 2022

Impact of Quaternary-Pumped Storage Hydropower on Frequency Response of U.S. Western Interconnection with High Renewable Penetrations

Preprint

Soumyadeep Nag,[1,2] Zerui Dong,[3] Jin Tan,[1] Jinho Kim,[3] Eduard Muljadi,[3] Kwang Y. Lee,[2] and Mark Jacobson[1]

1 National Renewable Energy Laboratory
2 Baylor University
3 Auburn University

Suggested Citation
Nag, Soumyadeep, Zerui Dong, Jin Tan, Jinho Kim, Eduard Muljadi, Kwang Y. Lee, and Mark Jacobson. 2022. *Impact of Quaternary-Pumped Storage Hydropower on Frequency Response of U.S. Western Interconnection with High Renewable Penetrations: Preprint*. Golden, CO: National Renewable Energy Laboratory. NREL/CP-6A40-81418. https://www.nrel.gov/docs/fy22osti/81418.pdf.

NREL is a national laboratory of the U.S. Department of Energy
Office of Energy Efficiency & Renewable Energy
Operated by the Alliance for Sustainable Energy, LLC

This report is available at no cost from the National Renewable Energy Laboratory (NREL) at www.nrel.gov/publications.

Contract No. DE-AC36-08GO28308

Conference Paper
NREL/CP-6A40-81418
July 2022

National Renewable Energy Laboratory
15013 Denver West Parkway
Golden, CO 80401
303-275-3000 • www.nrel.gov

NOTICE

This work was authored in part by the National Renewable Energy Laboratory, operated by Alliance for Sustainable Energy, LLC, for the U.S. Department of Energy (DOE) under Contract No. DE-AC36-08GO28308. Funding provided by the U.S Department of Energy Office of Energy Efficiency and Renewable Energy Water Power Technologies Office. The views expressed herein do not necessarily represent the views of the DOE or the U.S. Government.

Cover Photos by Dennis Schroeder: (clockwise, left to right) NREL 51934, NREL 45897, NREL 42160, NREL 45891, NREL 48097, NREL 46526.

Impact of Quaternary-Pumped Storage Hydropower on Frequency Response of U.S. Western Interconnection with High Renewable Penetrations

Soumyadeep Nag[1,2], Zerui Dong[3], Jin Tan[1], Jinho Kim[3], Eduard Muljadi[3], Kwang Y. Lee[2], Mark Jacobson[1]

1.Power System engineering Center, National Renewable Energy Laboratory, Golden, CO, USA

2. Dept. of Electrical and Computer Engineering, Baylor University, Waco, TX, USA

3. Dept. of Electrical and Computer Engineering, Auburn University, Auburn, AL, USA

***Abstract*— As renewable penetration increases in the United States, maintaining stability and reliability of low-inertia power grid by providing sufficient frequency control capability becomes a challenge. Advanced pumped storage hydro technologies (APSH) will be expected to play an important role for future grid as not only an energy supplier, but also as an ancillary services provider. This paper studies the impact of using quaternary pumped storage hydropower (Q-PSH), as one of the newly proposed APSH technology, to provide primary frequency response. To quantify the impact of Q-PSH on frequency response of the U.S. Western Interconnection, a user-defined dynamic model of Q-PSH is developed on the GE Positive Sequence Load Flow (PSLF) platform and is implemented in a set of detailed U.S. Western Electricity Coordination Council (WECC) planning cases in which renewable penetration levels are 20%, 40%, 60% and 80%. Simulation results show that Q-PSH can help improve frequency nadir and settling frequency comparing to the conventional PSH.**

***Index Terms* – Pumped storage hydro, quaternary pumped storage hydro, high renewable penetration, frequency response.**

I. INTRODUCTION

Variable renewable energy (VRE), like wind and solar photovoltaics (PVs), is being installed in an unprecedented rapid speed around the world. On one hand, the variability and uncertainty from the VRE could bring challenges on balancing the energy between generation and demand. On the other hand, the replacement of synchronous generators with these inverter-based resources (IBRs) are changing the dynamic characteristics of the bulk power systems, includes but not limited to physical inertia, short-circuit current, the primary and secondary frequency regulation capability, etc. Therefore, it poses challenges for maintaining stability, reliability, and resilience of power grid.

To further accommodate VRE in the power grid, energy storage has been identifying as a key technology to provide flexibility [1]. Pumped storage hydropower (PSH) technologies are becoming more valuable for its large capacity, the capability of long-term and short-term energy balancing and flexibility. In the United States, conventional pumped storage hydropower (C-PSH) is the widely used PSH technology. To maintain the stability and reliability of grid operation, C-PSH can provide primary frequency support and frequency regulation in the generating mode; however, these services cannot be provided during pumping mode, since it is operating at a fixed speed in the pumping mode.

In recent years, advanced pumped storage hydro (APSH) technologies have started to attract worldwide attention, because its high efficiency and ability to adjust power and provide the frequency ancillary services in the pumped mode [2]. Quaternary-PSH (Q-PSH), as one newly proposed APSH technology, has been developed by taking advantage of C-PSH and power electronic-based adjustable speed-PSH (AS-PSH). By leveraging the fast response capability of AS-PSH unit and physical inertia from the C-PSH unit in the quaternary configuration, Q-PSH can provide capability for both short-term energy balancing and fast power support in the future high renewable penetrated power system. We envision that this capability becomes more valuable as we further push the penetration of variable renewable generation. However, so far there is no publicly accessible study to quantify the benefit of using Q-PSH for grid operation in terms of frequency stability; in particular, to help different stakeholders (including policy makers, grid planners and operators and vendors) understand the role and value of new Q-PSH technology for the future high renewable scenarios.

This paper is to study the value of using Q-PSH for frequency support for an interconnection-level grid with high penetrations of renewable resources. The Western Interconnection electrical system in North America has been selected as a real large-scale test system for its rich hydropower resource and existing and planned PSH projects. The work presented here deals, specifically, with Q-PSH and investigates its impact on the frequency profile of the WECC system at different levels of renewable penetrations, up to 80%. The rest of this paper is organized as follows. Section II introduced the background of Q-PSH technology. Section III describes the modeling of Q-PSH. Section IV shows the impact study of Q-PSH on frequency response of Western Interconnection. The conclusion is given in Section V.

II. Advanced Pumped Storage Hydro

Q-PSH technology has been proposed to combine operational advantage of the adjustable speed pump of the AS-PSH and the hydraulic short circuit (HSC) of the T-PSH.

AS-PSH can be designed in two versions. The first version is where plant implements a doubly fed induction machine (DFIM) coupled with a reversible pump-turbine as shown in Fig. 1(a). In [3], author introduces the use of AS-PSH in generation mode efficiency enhancement for part-load conditions when a pump turbine is used. The work on frequency regulation provided by DFIM-based AS-PSH in the pumping mode is introduced in [4]. The smooth starting and fast braking using regenerative braking in AS-PSH can be observed in [5]. The second version is Full Converter AS-PSH (FC AS-PSH) which uses a fully fed converter system with a synchronous machine coupled with a reversible pump-turbine as shown in Fig. 1(b). This is a plant that implements a synchronous machine with the stator connected to the grid via a back-to-back voltage source converter and the required filter. The rotor is extended to provide excitation. In [6], author presents the dynamic modeling of fully fed AS-PSH and its fast frequency response.

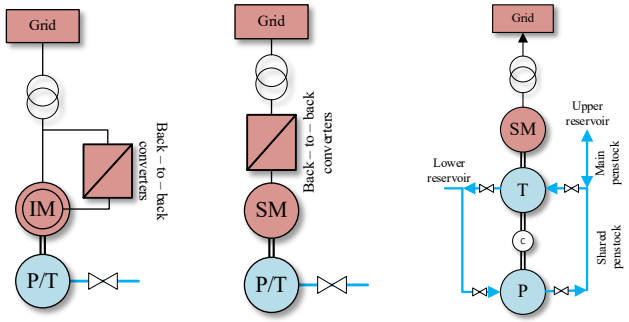

Fig 1. Functional diagram of (a) DFIG based AS-PSH (b) Synchronous machine based AS-PSH and (c) T-PSH.

T-PSH is an arrangement of a separate pump, a separate turbine and a synchronous machine on the same shaft to form a unit as displayed in Fig. 1(c). The turbine and pump can work separately or together to form a new operation mode so called HSC mode. Benefitting from the same shaft rotating direction of pump and turbine, T-PSH can change the operation mode quickly which make significant contributions to the frequency regulation [7].

Q-PSH combines the features of the AS-PSH and the T-PSH. As shown in Fig. 2, Q-PSH consists of two separate shafts, one for the pump-motor combination and another for the turbine-generator combination. Here, a full-sized back-to-back converter interfaces the pump-motor combination with the grid while the turbine-generator combination is directly connected to the grid. Synchronous machines are used for both, the adjustable-speed pump, and the generator. Benefiting from this mechanically independent hydraulic machine structure, the Q-PSH combines the benefits coming from AS-PSH and T-PSH as mentioned below:

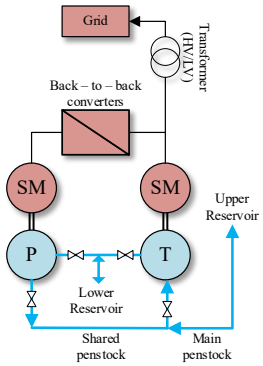

Fig 2. Functional diagram of Q-PSH

- Q-PSH can both extend the pump mode operating range and provide rapid response in pumping mode compared to T-PSH and AS-PSH which adds flexibility and responsiveness to the power system.
- In generating or idle mode, the converter in the pump unit can be acted as reactive power compensators. In pumping mode, the synchronous machine in the turbine unit can be operated as a synchronous condenser
- The separate shafts of Q-PSH configuration result in faster mode change times as compared to the T-PSH and AS-PSH configurations.

III. Quaternary PSH

A. Modelling Q-PSH

The relation between the flow rate of water and the difference in head for the turbine and pump can be given by:

$$\frac{dq_t}{dt} = \frac{H_t - h_t - h_l}{T_w} = \frac{\Delta h_t}{T_w} \quad (1a)$$

$$\frac{dq_p}{dt} = \frac{-[H_p - h_p - h_l]}{T_w} = \frac{\Delta h_p}{T_w} \quad (1a)$$

Here H_t, H_p, h, and h_l define the static head for the turbine, static head for the pump, head at turbine entrance, and head loss due to friction as $h_l = f_p Q^2$, (where Q can be the flow rate of water for the turbine or pump) and T_w is the water starting time constant. Since the turbine and pump are connected, it is required that we model the interaction between the two. According to [8], the hydraulic dynamics for the pump and turbine and their mutual connection can be given by:

$$\begin{bmatrix} T_{w\_tt} & T_{w\_tp} \\ T_{w\_pt} & T_{w\_pp} \end{bmatrix} \begin{bmatrix} \frac{dq_t}{dt} \\ \frac{dq_p}{dt} \end{bmatrix} = \begin{bmatrix} \Delta h_t \\ \Delta h_p \end{bmatrix} \quad (2)$$

where, T_{w_tt}, T_{w_pp} are the water time constants for the entire penstock length of the turbine and the pump; T_{w_tp}, T_{w_pt} are the water time constants for the shared-penstock length from the turbine to the pump or from the pump to the turbine. The discharge and the head for the turbine is given by,

$$q_t = G_t \sqrt{h_t} \quad (3)$$

where, G_t is the turbine gate and h_t is the head at turbine inlet. For the pump model, the equation (3) needs to be modified. Unlike the turbine gate, the pump gate G_p can either be fully closed or fully open and hence is not considered as a control variable for the pump model. Instead, the speed of the pump can be controlled. Thus, for the pump the relationship between flow and head at the pump exit is expressed as a function of speed instead of gate as:

$$h_p = a_0\omega^2 + a_1\omega|q_p| + a_2q_p^2 \quad (4)$$

where, a_0, a_1 and a_2 are coefficients for curve fitting, ω is the mechanical speed of the pump shaft, simulated by:

$$2H\frac{d\omega}{dt} = P_m - P_e - D\omega \quad (5)$$

Here, P_m, P_e, D, and H are mechanical power, electrical power, damping and inertia constants, respectively. The mechanical power for both pump and turbine are given by:

$$P_m = \frac{\rho ghq}{\eta} \quad (6)$$

where, h and q can be pump or turbine instantaneous head and discharge, respectively, and η is the efficiency of the pump or turbine.

B. Control of Q-PSH

To control the operating mode of Q-PSH and distribute the power order to both turbine unit and pump unit, a distribution function is designed as [9]:

$$\begin{cases} P_{ord\_p} = -K_{d\_p} \times |P_{demd}| \\ P_{ord\_t} = K_{d\_t} \times |P_{demd}| \end{cases} \quad where\ K_{d\_p}, K_{d\_t} \epsilon\ [0,1] \quad (7)$$

where, K_{d_p} and K_{d_t} are the power distribution coefficients for the pump and turbine, part respectively where, K_{d_p} and K_{d_t} $\in$[0,1] is the total power demanded from the unit. The value of the coefficients can be set by the operator according to a schedule, but the coefficients obey the condition that, $K_{d\_t} = 1 - K_{d\_p}$. The pump power order is given to the pump's converter control according to which the controller generates and tracks a current reference. This result in the change in electrical power that consequently alters the speed of the system. The turbine power order is given to the hydraulic governor which regulates the turbine inlet valve while maintaining synchronous speed. The control system for the Q-PSH is represented in Fig. 3.

Primary control signals form the droop can be generated using the system frequency deviation for both the conventional turbine governor and the pump converter. The inertia and primary frequency controller have been modelled and implemented as:

$$\Delta P_i = DB_iK_i\frac{1}{1+sT_i}\frac{sT_{wout}}{1+sT_{wout}}\Delta f \quad (8)$$

$$\Delta P_g = DB_gK_g\frac{1}{1+sT_g}\frac{1+sT_z}{1+sT_p}\Delta f \quad (9)$$

In (8) and (9) a dead-band DB_i and DB_g is used to reduce control activity, followed by a gain K_i and K_g for amplification and a low pass filter to eliminate noise. The washout filter in the inertia control in (8) allows it to respond only to fast changes in frequency, while the lag compensator in the primary frequency controller allows it to respond to the slow changes in frequency and compensate for controller and sensor delay.

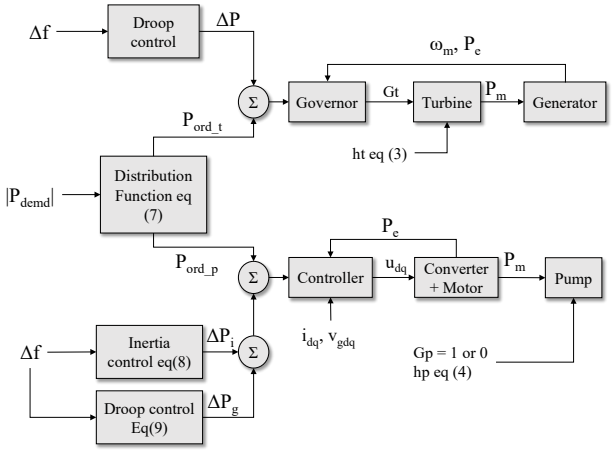

Fig. 3. Control system overview for Q-PSH.

To model the Q-PSH system in the GE PSLF platform, the user-defined and existing models are used. The hydraulic, mechanical and control system in the Q-PSH is modeled by an EPCL user-defined model with the name EPCTRB [9]. For the machines in turbine and pump units, the existing models in the library are used. For the synchronous machine in the turbine unit, the salient pole synchronous generator model GENSAL and IEEE Type DC1A exciter model 'IEEET1' are used. The pump motor and converter system in the pump unit are modeled with GEWTG, while its real and reactive power tracking controller are modeled with EWTGFC [10]. The references for machines in pump unit and turbine are given by the user-defined governor model. Similar to other commercially available software, in the PSLF all of the above components (user-defined or pre-existing) and their parameters can be added to the dynamic data file as one component.

IV. Simulation Results and Discussion

A. Test System – Detailed WECC System

This work considers the WECC 2022 light spring case (2022LSP) system where the system conditions represent a low load and a planned amount of high renewable penetration. Also, in the spring of 2015 four generation trip events were recorded which eased the process of model verification. Results from the model verification displayed that the WECC model was successfully able to capture the time-domain dynamics of system frequency. Detailed results can be found in [11].

The test system consists of 19000+ busses, 4000+ generators, and is divided among 21 areas, 424 zones and 492 owners. Here, not all generators are equipped with governor systems e.g., nuclear and a few coal-based plants. Most of the governor response is derived from hydro, combined-cycle, and gas-turbine units. The main governor turbine models used in the system are GGOV1, HYGOV, IEEEG1, IEEEG3, HYG3, HYGOV4, GPWSCC. The main generator models used were GENROU, GENTPJ, and GENTPF with IEEET1 as the main excitation system [12].

B. *Development of High Renewbale Penetration Scenarios*

The renewable energy (RE) penetration of 20, 40, 60% and 80% scenarios have been developed by keeping the wind power constant at 15% and varying the rooftop PV penetration as shown in table I. Rooftop PV and utility-scale PV have different behaviors [12].

Rooftop PV technical potential-based method and NSRDB based data were simultaneously used to calculate the suitable space and insolation available at a zip code, respectively. In brief, rooftop PV technical potential-based method processes Light Detection and Ranging data and building footprint data which are analyzed for shading, tilt, and Azimuth to determine the suitability of rooftop area for PV [13, 14]. The NSRDB is an open source NREL-built database that provides the solar irradiation data that can be further be modified by using the geographical and weather information of the area of interest [15].

TABLE I. SYSTEM INERTIA FOR DIFFERENT SIMULATION CASES [16]

Case	System Inertia	Wind Penetration	PV Penetration	Total Penetration
20%	3.02	14.36%	1.73%	21.03%
40%	2.21	14.36%	22.73%	42.02%
60%	1.93	14.53%	42.28%	60.16%
80%	0.93	14.53%	61.16%	80.61%

C. *Baseline Analysis*

For the baseline analysis, the WECC system was considered with C-PSH installed at respective locations, which amounted to 4147MW. The detailed information of these C-PSH can be found in [16]. The baseline analysis provides a sense of the problem at hand and in fact verifies the assumption that higher penetrations of renewables will reduce system inertia and cause larger deviations in system state variables. At 10 seconds, a plant (2.7 GW) trip is simulated, and the system experiences a frequency transient due to the sudden imbalance of real power. The frequency profile, as in Fig. 4, displays a lower frequency nadir and settling frequency as the penetration level changes from 20% to 80%. The 2022LSP case considers, the total output of -2553MW at the time the disturbance was applied.

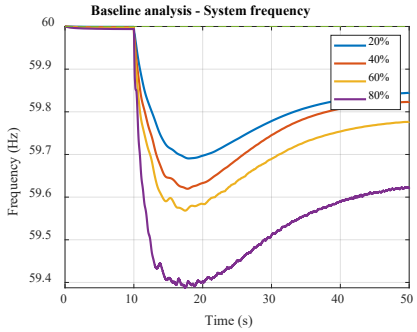

Fig. 4. WECC System responses to a plant trip event under 20%, 40%, 60% and 80% renewable penetration.

D. *Integration of Q-PSH*

To test the impact of Q-PSH, several existing C-PSH units in the system were replaced by the Q-PSH. The Q-PSH governor was developed using user-defined model in GE's PSLF [16] platform. While replacing the existing C-PSH unit, the generator, exciter, and associated stabilizer models were left unaltered to retain a level of certainty.

E. *Impact of Q-PSH with Different Renewable Penetration Levels*

After replacing the selected C-PSH with Q-PSH operating in HSC mode in the WECC system, the same event as in the baseline case was applied at 10 seconds in each level of penetration case. From Fig. 5(a) and 6(a) we can conclude that a) the initial rapid response from the converters of the Q-PSH helps improve the frequency nadir by 0.1 Hz and 0.25 Hz, b) the joint response from the pump and turbine improves the settling frequency by 0.05 Hz and 0.18 Hz, and c) the rate of change of frequency is considerably reduced close to the frequency nadir.

Fig. 5(b) and 6(b) shows the real power contribution from all Q-PSH units in the WECC system and verifies the capabilities of Q-PSH that results in the above-mentioned conclusions. From these figures it can be observed that, before 10 seconds, system operates normally at desired frequency. As soon as the disturbance is applied at 10 seconds, system frequency drops and rapid inertial response from the C-PSH and Q-PSH is realized. Clearly, after the event at 10 seconds, with the combined action of the inverter-based inertia control and synchronous machine inertia, the Q-PSH has greater inertial response compared to the C-PSH. Later, the effect of droop control of both the pump and turbine results in significant reduction in the power consumed. In the 80% renewable penetration case, it can be observed from the Fig. 6(b) that the inertial response is greater than that in Fig 5(b) which results from the sharp ROCOF at higher renewable penetrations. Also, at 80% penetration, the frequency settles lower than that in the 20% case which elevates the contribution from the primary control of the Q-PSH.

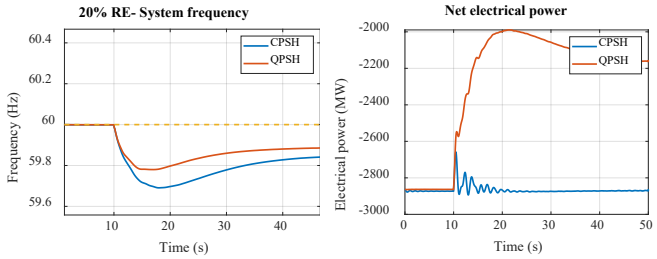

(a) (b)

Fig. 5. Analysis of WECC system (a) frequency and (b) power response with Q-PSH vs. with C-PSH under 20% RE penetration.

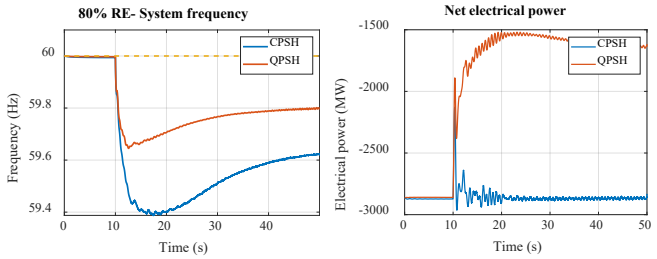

(a) (b)

Fig. 6. Analysis of WECC system (a) frequency and (b) power response with Q-PSH vs. with C-PSH under 80% RE penetration.

Fig. 7 breaks up one Q-PSH plant's response and illustrates the dynamics of the pump and generator power output. Fig. 8 shows that with Q-PSH more than 80% renewables can be hosted in the same network from a dynamic stability standpoint as the frequency nadir is above the 59.5 Hz mark, whereas frequency nadir in the C-PSH 80% penetration case is below 59.5 Hz. The settling frequency also shows better values which is mainly due to the added relief from the primary frequency response of both pump and generator which is only possible with the Q-PSH.

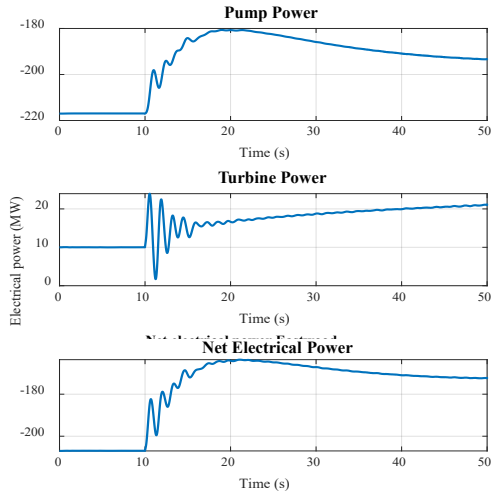

Fig. 7. Electrical power output from pump, turbine and combined.

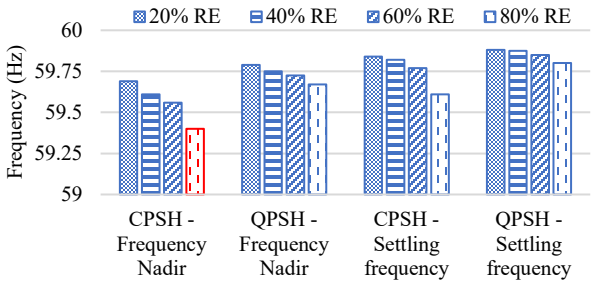

Fig. 8. Summary chart for system frequency nadir and setling frequency

V. Conclusion

This paper has studied the impacts of Q-PSH on frequency response of the U.S. Western Interconnection under 20%, 40%, 60% and 80% renewable penetration levels, during the pump mode operation. Compared to the C-PSH, Q-PSH in HSC mode shows higher frequency nadir, higher settling frequency and slower ROCOF. This is possible due to the rapid response of the converter-based pump combined with the HSC based response from the turbine of the Q-PSH. As a result, the frequency nadir of the system is maintained above 59.5Hz even under 80% renewable penetration.

Acknowledgments

This work was authored in part by Alliance for Sustainable Energy, LLC, the manager and operator of the National Renewable Energy Laboratory for the U.S. Department of Energy (DOE) under Contract No. DE-AC36-08GO28308. Funding provided by the U.S. Department of Energy Office of Energy Efficiency and Renewable Energy Water Power Technologies Office. The views expressed in the article do not necessarily represent the views of the DOE or the U.S. Government. The U.S. Government retains and the publisher, by accepting the article for publication, acknowledges that the U.S. Government retains a nonexclusive, paid-up, irrevocable, worldwide license to publish or reproduce the published form of this work, or allow others to do so, for U.S. Government purposes.

References

[1] J. P. Barton and D. G. Infield, "Energy storage and its use with intermittent renewable energy," in IEEE Transactions on Energy Conversion, vol. 19, no. 2, pp. 441-448, June 2004, doi: 10.1109/TEC.2003.822305.

[2] A. Botterud, T. Levin and V. Koritarov, "Pumped Storage Hydropower: Benefits for Grid Reliability and Integration of Variable Renewable Energy", Argonne National Laboratory, Chicago, 2014.

[3] S. Nag and K. Y. Lee, "DFIM-Based Variable Speed Operation of Pump-Turbines for Efficiency Improvement", IFAC-PapersOnLine, vol. 51, no. 28, pp. 708-713, 2018. Available: 10.1016/j.ifacol.2018.11.788.

[4] S. Nag, K. Y. Lee, D. Suchitra, and V. Mediratta, "Load Frequency Control through DFIM-Based Pumped Storage Hydro", in IEEE PES GM, Atlanta, GO, 2019.

[5] Joseph, Anto, Raghu Selvaraj, and S. V. Appa Sarma. "Starting and Braking of a Large Variable Speed Hydrogenerating Unit Subjected to Converter and Sensor Faults," IEEE Transactions on Industry Applications 54, no. 4 (2018): 11.

[6] Z. Dong, E. Muljadi, J. Kim and R. M. Nelms, "Dynamic Modeling of Full Converter Adjustable-speed Pumped Storage Hydropower (FC AS-PSH)," 2020 IEEE Power & Energy Society General Meeting (PESGM), 2020, pp. 1-8, doi: 10.1109/PESGM41954.2020.9281806.

[7] Dong, Zerui, Jin Tan, Antoine St-Hilaire, Eduard Muljadi, David Corbus, Robert Nelms, and Mark Jacobson. "Modelling and simulation of ternary pumped storage hydropower for power system studies." IET Generation, Transmission & Distribution (2019).

[8] Z. Dong, R. Nelms, E. Muljadi, J. Tan, V. Gevorgian and M. Jacobson, "Development of dynamic model of a ternary pumped storage hydropower plant," 2018 13th IEEE Conference on Industrial Electronics and Applications (ICIEA), Wuhan, 2018, pp. 656-661. doi: 10.1109/ICIEA.2018.8397796

[9] Z. Dong et al., "Developing of Quaternary Pumped Storage Hydropower for Dynamic Studies," in IEEE Transactions on Sustainable Energy, vol. 11, no. 4, pp. 2870-2878, Oct. 2020, doi: 10.1109/TSTE.2020.2980585.

[10] G. Concorda, "PSLF user's manual, ver 18," ed, 2013.

[11] N. W. Miller, M. Shao, R. D'aquila, S. Pajic, and K. Clark, "Frequency Response of the US Eastern Interconnection Under Conditions of High Wind and Solar Generation," in 2015 Seventh Annual IEEE Green Technologies Conference, 2015, pp. 21-28.

[12] J. Tan, Y. Zhang, S. Veda, T. Elgindy, and Y. Liu, "Developing High PV Penetration Cases for Frequency Response Study of U.S. Western Interconnection," *2017 Ninth Annual IEEE Green Technologies Conference (GreenTech)*, Denver, CO, 2017, pp. 304-311. doi: 10.1109/GreenTech.2017.51

[13] "Solar Industry Research Data | SEIA", SEIA, 2019. [Online]. Available: https://www.seia.org/solar-industry-research-data.

[14] P. Gagnon, R. Margolis, J. Melius, C. Phillips, and R. Elmore, "Rooftop Solar Photovoltaic Technical Potential in the United States: A Detailed Assessment," Rep. No. NREL/TP-6A20-65298). Retrieved March, vol. 30, p. 2016, 2016.

[15] "NSRDB Data Viewer", Maps.nrel.gov, 2019. [Online]. Available: https://maps.nrel.gov/nsrdb-viewer/.

[16] Z. Dong, J. Tan, E. Muljadi, R. Nelms and M. Jacobson, "Impacts of Ternary-Pumped Storage Hydropower on U.S. Western Interconenction with Extremely High Renewable Penetrations," 2019 IEEE Power & Energy Society General Meeting (PESGM), 2019, pp. 1-5, doi: 10.1109/PESGM40551.2019.8973787.

[17] "Energy Management System | PSLF | GE Energy Consulting", Geenergyconsulting.com, 2019. [Online]. Available: https://www.geenergyconsulting.com/practice-area/software-products/pslf.